

Analysis of LSFD and USFD Distressed during 1971 and 1994 Earthquake considering Soil Anisotropy

R. Singh¹ and D. Roy²

ABSTRACT

Using the commercial finite element software, the response of Lower San Fernando Dam (LSFD) and Upper Fernando Dam (USFD) distressed during 1971 San Fernando earthquake and 1994 Northridge earthquake are analyzed in terms of total stress employing an equivalent static finite element model. An Drucker-Prager (DP) elastic perfectly plastic stress-strain model with 2-D plane-strain and four-node solid elements were used in the numerical model which is developed in ABAQUS Explicit (ver. 6.8) computer program. In the first step of the finite element analysis, the numerical model was brought into equilibrium under self-weight using drained shear strength and deformation parameters. In the second step of deformation modeling, applicable shear strength parameters were reset to represent the rapid loading condition with shear strength parameters. The horizontal and vertical deformations obtained from the finite element analysis were found to compare reasonably with observed post-earthquake deformation patterns for both of the embankments.

Introduction

Upstream slope of Lower San Fernando dam (LSFD) failed immediately after the 1971 San Fernando earthquake of magnitude 6.6 (M_w). Peak horizontal ground acceleration (a_{max}) at the dam site reached 0.5g caused reason due to a large volume of hydraulic fill within the dam body to liquefy, which, in turn precipitated in the flow failure resulting in horizontal and vertical displacements as large as 61 m and 15 m, respectively (Seed et al. 1975). LSFD rehabilitated after the 1971 failure was shaken in 1994 by the Northridge earthquake 6.9 (M_w). Although the dam site a_{max} during this event was only 0.32g, liquefaction was triggered underneath the lower portion of the downstream slope leads to the development of deformations 0.15 m horizontal and 0.10 m vertical respectively (Bardet and Davis 1996). During 1994, the deformations probably resulted from liquefaction related loss of shear strength underneath the lower part of the downstream slope (Bardet and Davis 1996).

Upper San Fernando dam suffered distress during the 1971 San Fernando earthquake (M_w 6.6; dam site a_{max} between 0.55g and 0.60g). Liquefaction was triggered in this event within saturated hydraulic fill. Horizontal and vertical deformations of the dam measured 1.7 m and 1.0 m, respectively, and longitudinal cracks with offsets were observed in the full length of the upstream face of the dam indicates the stability of the dam to be marginal. Upper San Fernando dam rehabilitated after the 1971 event endured the 1994 Northridge earthquake (M_w 6.9 and dam site a_{max} 0.32g) with relatively minor distress despite triggering of liquefaction. Several small

¹R. Singh, Department of Civil Engineering, UEC, Ujjain, MP, India, raghvendr@gmail.com

²D Roy, Department of Civil Engineering, IIT Kharagpur, WB, India, debasis@civil.iitkgp.ernet.in

cracks were developed after this event mainly in the upstream portion of the dam (Bardet and Davis 1996).

In this paper, Lower San Fernando Dam (LSFD) and Upper Fernando Dam (USFD) during 1971 San Fernando earthquake and 1994 Northridge are analyzed in terms of total stress in a equivalent static finite element analysis with Drucker-Prager (DP) elastic- perfectly plastic stress-strain model using commercial finite element software package ABAQUS Explicit (ver. 6.8).

Soil Anisotropy Formulation

Generally the design of the earth structures like dams and embankments constructed with/or underlain by saturated non plastic soils are generally governed by yield and residual shear strength parameters of the soils. Yield and residual shear strengths are often estimated directly available correlation between yield or residual shear strengths and penetration resistances from the back analysis of pre and post failure geometries of earth structures that suffered varying degrees of distress resulting from rapid or seismic loading. Yield shear strengths of saturated non plastic soils are estimated based on the assumption of inherently isotropic soil behavior, however saturated non plastic soils exhibit strong inherent anisotropy during rapid loading. By these limitations, a relationship between yield shear strengths and penetration resistances were proposed by Singh, (2012) considering the anisotropic soil behavior and from back analysis of thirty two case histories. Correlations between yield shear strengths and compressibility and stress level corrected cone tip resistances are presented in Figure 1a, and are incorporated in the finite element modeling.

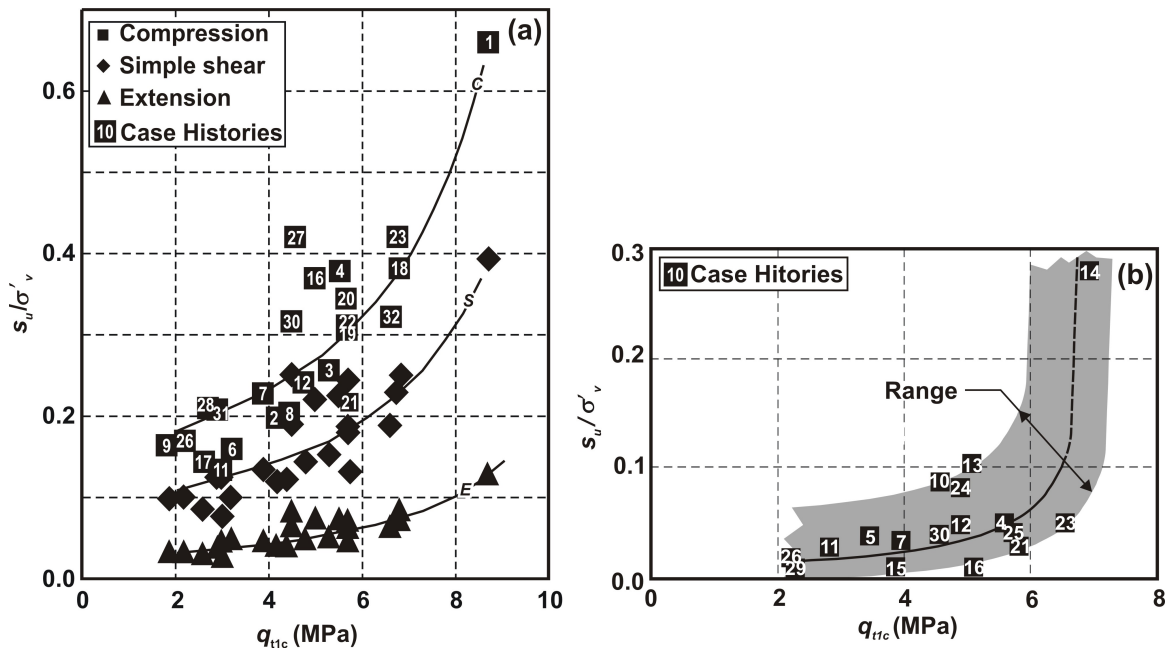


Figure 1a,b. Relationships for yield and residual shear strengths (modified from Singh, 2012)

Similarly, because the post deformation shear strengths has small effect on anisotropy during the rapid loading (Jefferies and Been, 2006) and the behavior of the failed material depends on various parameters (e.g. viscous and frictional resistance, strain energy, void redistribution and loss of potential energy, flexibility) during failure. After considering these effects, Singh, (2012) proposed relationships between residual shear strengths and penetration resistances using a procedure based on energy approach and using the back analysis of seventeen case histories distressed during rapid and seismic loadings. Correlations between residual shear strengths and compressibility and stress level corrected cone tip resistances are presented in Figure 1b, and are incorporated in the finite element modeling. For the validation of correlations for residual shear strengths proposed by Singh (2012), a comparison with Stark and Mesri (1992) and Idriss and Boulanger (2008) are presented in Figure 2 and these comparisons indicates that the range and pattern of the residual shear strengths with stress normalized penetration resistances presented by Stark and Mesri (1992) and by Idriss and Boulanger (2008) are similar to range of Singh (2012).

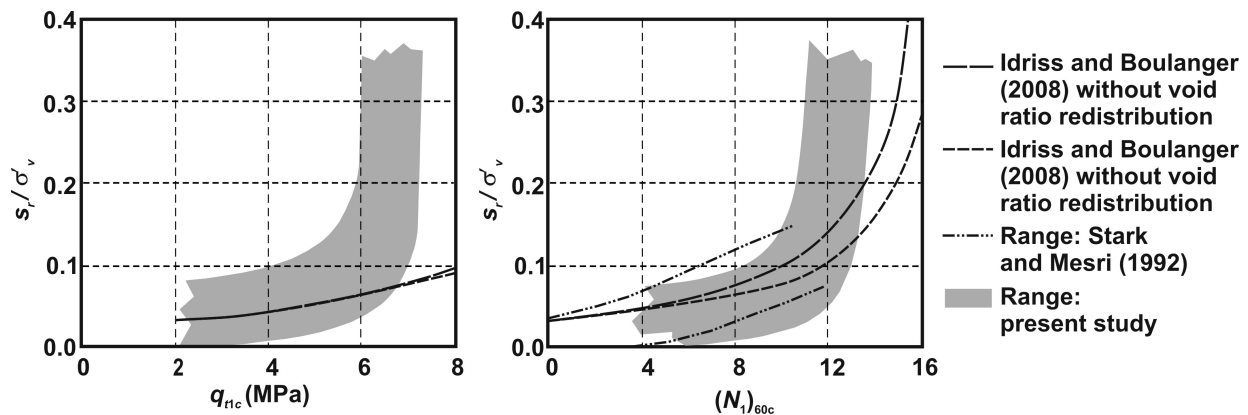


Figure 2. Comparison of residual shear strengths

Finite Element Modeling

The numerical models are developed for all four dam case histories using the pre failure geometries in the commercial finite element software package ABAQUS Explicit (ver. 6.8). The finite element analysis is based on total stress employing Drucker-Prager (DP) elastic-perfectly plastic stress-strain model. 2-D plane-strain and four-node solid elements were used in the analyses. In the analysis, the horizontal bottom boundary was restrained to move only horizontally and the vertical boundaries were restrained to move only in the vertical direction. A general procedure adopted for the finite element analysis is presented as a flow chart presented in Figure 3. The liquefiable soils the input shear strengths in the second step of deformation modeling were also scaled up by a factor of 2.0 to account of the velocity dependent component of shear strength (deAlba and Bellestero, 2006). In analyses, contractive but non-liquefied soils mechanical behavior was assumed to be anisotropic, while liquefied material behavior was assumed to be isotropic. The shear strength parameters were estimated from cone tip resistance according to Figure 1a,b. Shear modulus estimated from correlations based on penetration resistance (Lunne et al. 1997) for non liquefied soils. For liquefiable soils, the shear modulus was reset to 1/100th of the corresponding pre liquefaction value (Lunne et al. 1997) in the second step of deformation modeling.

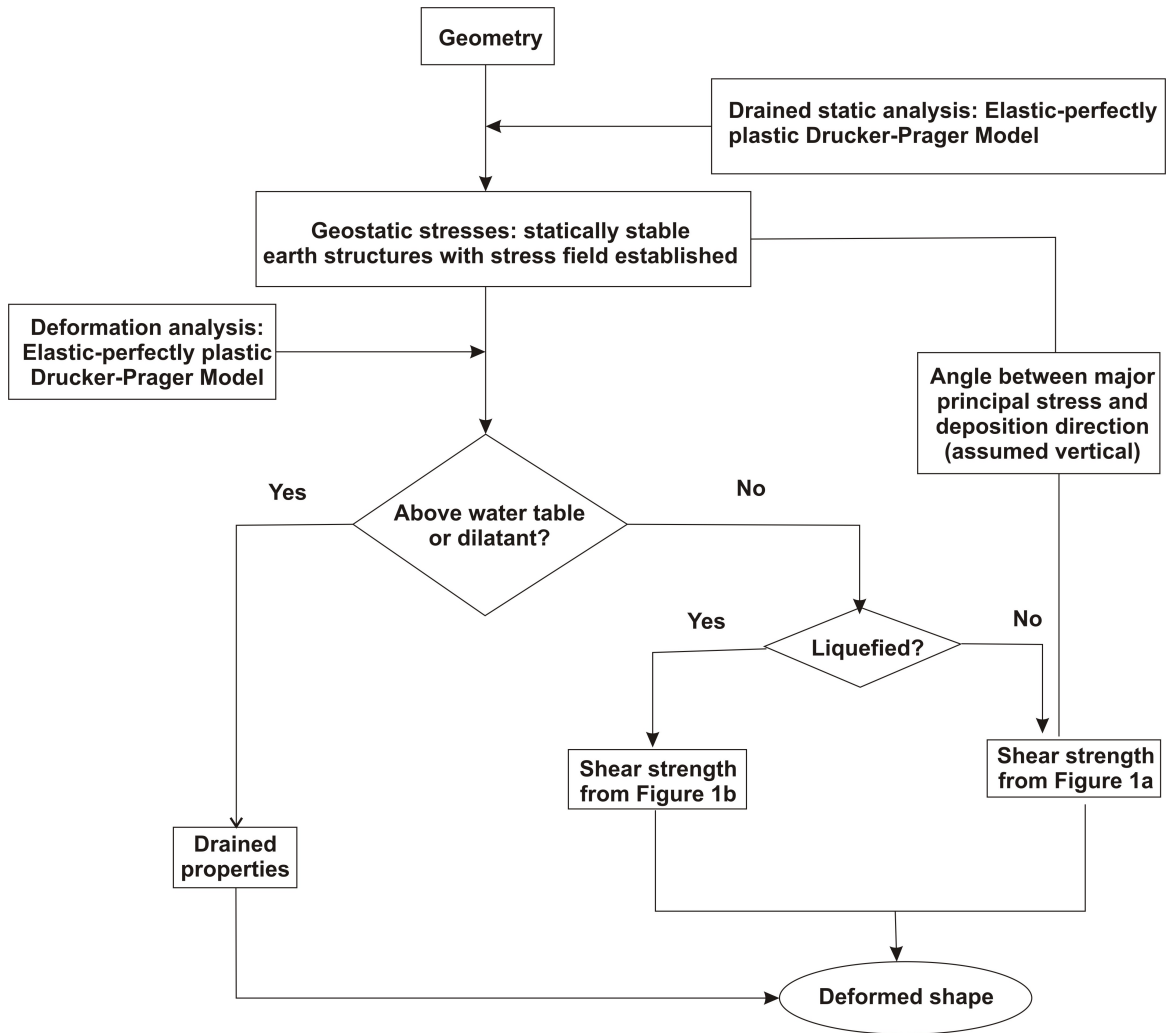


Figure 3. Flow chart for finite element analysis

Estimation of Deformation: LSFD 1971 San Fernando Earthquake

Since in 1971 the dam suffered large deformations after the recession of the earthquake rather than during the event (Seed et al. 1975), the numerical model no earthquake ground motion was used in second step of the analysis. The hydraulically placed sand characterized with normalized cone tip resistance, q_{tl} of about 4.5 MPa. The corresponding q_{tlc} is 6.8 MPa assuming medium compressibility of soil grains.

For the soils with q_{tlc} more than 9.75 MPa or soils above water table, the drained values of friction angle were used. Below the water table, for the given value of q_{tlc} , 6.8 MPa, the residual shear strength ratio for the liquefied hydraulic fill layer was computed 0.120 from Figure 1b. The input soil properties (unit weight, cohesion and degree of internal friction) used in this analysis taken from Seed et al. (1975) and are listed in Table 1. Values of poisson ratio and young's modulus are taken from generic relationships. The 1st and 2nd entries in columns 2 to 7 represented in Table 1 used in stage 1 (establishing geostatic stress) and stage 2 (deformation modeling) of analysis. The horizontal displacement (U_1) and the deformation pattern obtained from analysis are presented in Figure 4. Maximum deformations obtained from finite element analysis are somewhat smaller than the observed value; the large deformations obtained analytically are in agreement with the flow failure observed in 1971 earthquake.

Table 1. Soil parameters for LSFD 1971 analysis

Soil	$\gamma^{(1)}$, kN/m ³	E , MPa	μ	c , kPa	ϕ deg.	s_u/σ'_v
Rolled fill	19.2, 19.2	98, 98	0.22, 0.22	0, 0	37°, -	-, -
D/S hyd. fill (above)	19.2, 19.2	73, 73	0.22, 0.22	0, 0	32°, 32°	-, -
D/S hyd. fill (below)	19.2, 19.2	73, 73	0.22, 0.49	0, 0	32°, -	-, 0.23 ⁽²⁾
Upstream hyd. fill	19.2, 19.2	73, 0.73	0.22, 0.22	1, 1	32°, -	-, 0.11
Clay core	16.0, 16.0	68, 68	0.40, 0.40	39, 39	-, -	-, -
Shale	22.5, 22.5	85, 85	0.22, 0.22	0, 0	42°, 42°	-, -
Alluvium	22.3, 22.3	85, 85	0.22, 0.22	0, 0	40°, 40°	-, -

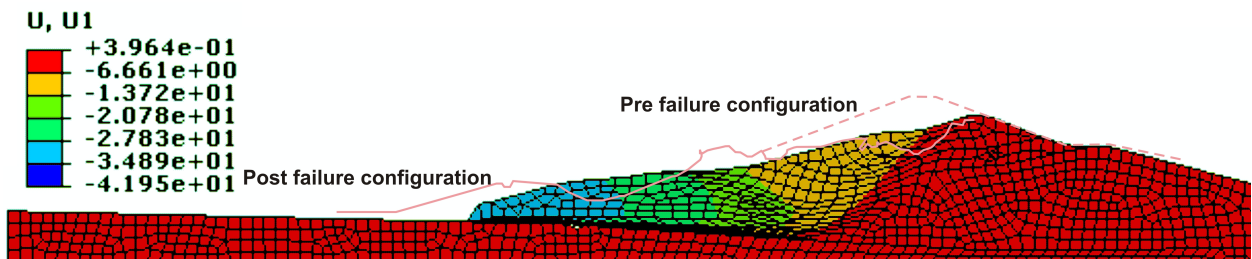


Figure 4. Horizontal deformation of LSFD 1971 earthquake

Estimation of Deformation: LSFD 1994 Northridge Earthquake

Since the deformations likely to have developed after liquefaction, a phenomenon leading to a significant increase in material damping, inertia forces related to earthquake acceleration were ignored in the step 2 of the analysis. The input material properties of different zoning of material listed in Table 2 were estimated from published penetration resistance.

The geostatic stress distribution obtained the first step of the analysis is shown in Figure 3. The deformation pattern obtained from the second step of analysis using shear strength correlations developed in this study are presented in Figure 1a,b. The 1st and 2nd entries in columns 2 to 7 represented in Table 2 used in stage 1 (establishing geostatic stress) and stage 2 (deformation modeling) of analysis. The maximum deformations obtained from finite element analysis (Figure 5) are somewhat exceeded the observed values reported in Bardet and Davis (1996), relatively small deformations obtained analytically are in agreement with the stable performance of LSFD observed in 1994.

Table 2. Soil parameters for LSFD 1994 analysis

Soil	$\gamma^{(1)}$, kN/m ³	E , MPa	μ	c , kPa	ϕ , deg.	s_u/σ'_v
Berm	19.2, 19.2	98, 98	0.22, 0.22	0, 0	35°, –	–, –
Compacted fill	20.3, 20.3	98, 98	0.22, 0.22	0, 0	37°, –	–, –
Hyd. fill	19.2, 19.2	73, 73	0.22, 0.22	0, 0	35°, –	–, –
Hyd. fill (NL)	19.2, 19.2	73, 73	0.22, 0.49	0, 0	35°, –	–, 0.19 ⁽²⁾
Hyd. fill (L)	19.2, 19.2	73, 0.73	0.22, 0.49	0, 0	35°, –	–, 0.08
Clay core	19.2, 19.2	42, 42	0.40, 0.40	39, 39	–, –	–, –
Alluvium	22.0, 22.0	85, 85	0.22, 0.22	0, 0	40°, –	–, –

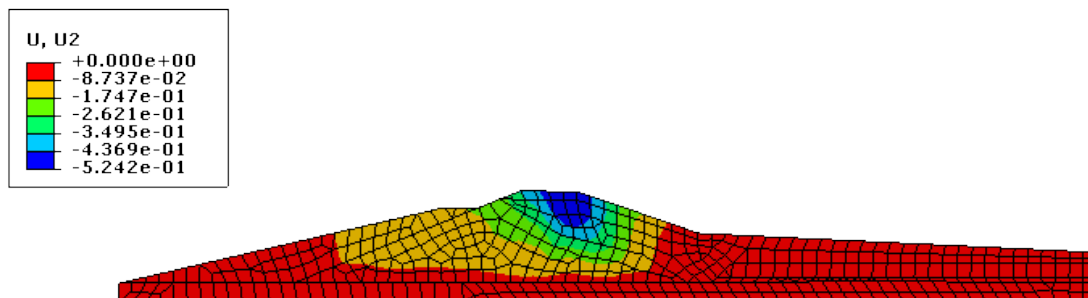


Figure 5. Vertical deformation of LSFD 1971 earthquake

Estimation of Deformation: USFD 1971 San Fernando Earthquake

The San Fernando earthquake of 1971 also led to the development of liquefaction within the hydraulic fill within the body of Upper San Fernando dam. However, the resulting deformations were relatively small in that event with the maximum deformation of 3.2 m developing in the horizontal direction. Since the distress developed after the recession of ground motion (Huynh et al. 2006), in finite element modeling earthquake time history was not considered. The average q_{tl} the corresponding q_{tlc} within the hydraulic fill layer were 3.9 MPa and 6.2 MPa, respectively, assuming medium grain compressibility (Seed et al. 1975). The input soil properties (unit weight, cohesion and degree of internal friction) used in this analysis taken from Seed et al. (1975) and are listed in Table 3. Values of poison ratio and young's modulus are taken from generic relationships. The horizontal displacement (U_1) obtained from the second step of analysis using shear strength correlations developed in this study are presented in Figure 6. The computed deformations were found to compare reasonably with observations.

Table 3. Soil parameters for USFD 1971 analysis

Soil	$\gamma^{(1)}$, kN/m ³	E , MPa	μ	c , kPa	ϕ , deg.	s_u/σ'_v
Rolled fill	22.0, 22.0	98, 98	0.22, 0.22	0, 0	37°, -	-, -
Hyd. Fill (above)	19.2, 19.2	73, 73	0.22, 0.22	0, 0	37°, 37°	-, -
Hyd. fill (NL)	19.2, 19.2	73, 73	0.22, 0.49	0, 0	37°, -	-, 0.23 ⁽²⁾
Hyd. fill (L)	19.2, 19.2	73, 0.73	0.22, 0.49	0.5	37°, -	-, 0.11
Clay core	19.2, 19.2	42, 42	0.40, 0.40	-, -	37°, 37°	-, -
Alluvium	20.3, 20.3	85, 85	0.22, 0.22	0.0	40°, -	-, -

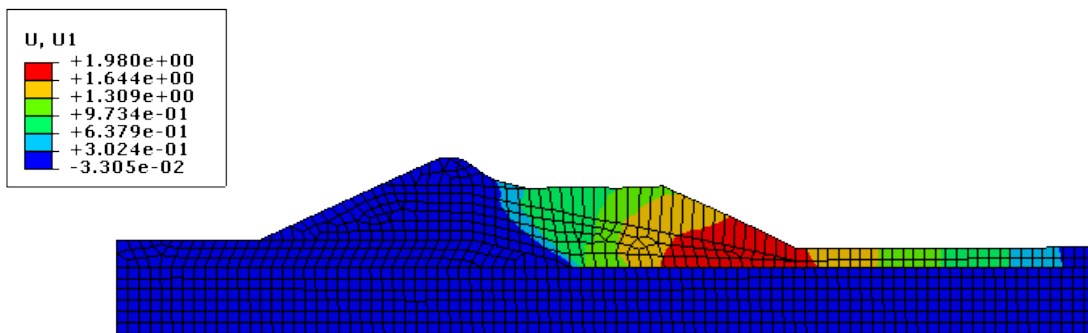


Figure 6. Horizontal deformation of USFD 1971 earthquake

Estimation of Deformation: USFD Northridge 1994 Earthquake

USFD rehabilitated after the 1971 event endured the 1994 Northridge earthquake (M_w 6.9 and dam site a_{max} 0.32g) with relatively minor distress despite triggering of liquefaction. Several small cracks developed after this event mainly in the upstream portion of the dam (Bardet and Davis 1996). These observations are indicative of liquefaction of portions of saturated hydraulic fill. The average q_{tl} the corresponding q_{tlc} within the upstream side hydraulic fill layer were 3.6 MPa and 5.0 MPa, respectively, assuming medium grain compressibility (inferred from the downstream CPT data reported by Bardet and Davis 1996). Since in 1994 the deformations probably resulted from liquefaction near the dam base and after the recession of the earthquake rather than during the event (Bardet and Davis 1996), the numerical model no earthquake ground motion was used in step 2 of the analysis. The input material properties listed in Table 4 were estimated from Figure 1a,b and also from published penetration resistance for different material zones. The deformation pattern obtained from the second step of analysis using shear strength correlations developed in this study are presented in Figure 7. The maximum deformations obtained from finite element analysis were found to compare reasonably with the observed values reported in Bardet and Davis (1996). The 1st and 2nd entries in columns 2 to 7 represented in Table 4 used in stage 1 (establishing geostatic stress) and stage 2 (deformation modeling) of analysis.

Table 4. Soil parameters for USFD 1994 analysis

Soil	$\gamma^{(1)}$, kN/m ³	E , MPa	μ	c , kPa	ϕ	s_u/σ'_v
Rolled fill	22.0, 22.0	98, 98	0.22, 0.22	0, 0	37°, -	-, -
Hydraulic fill	19.2, 19.2	98, 98	0.22, 0.22	0, 0	37°, -	-, -
Clay core	19.2, 19.2	42, 42	0.49, 0.49	0, 0	38°, -	-, -
Non liquefied zone	19.2, 19.2	73, 73	0.22, 0.49	0, 0	-, -	-, 0.18 ⁽²⁾
Liquefied zone	19.2, 19.2	73, 0.73	0.22, 0.49	0, 0	-, -	-, 0.05
Alluvium	20.3, 20.3	85, 85	0.22, 0.22	0, 0	40°, -	-, -

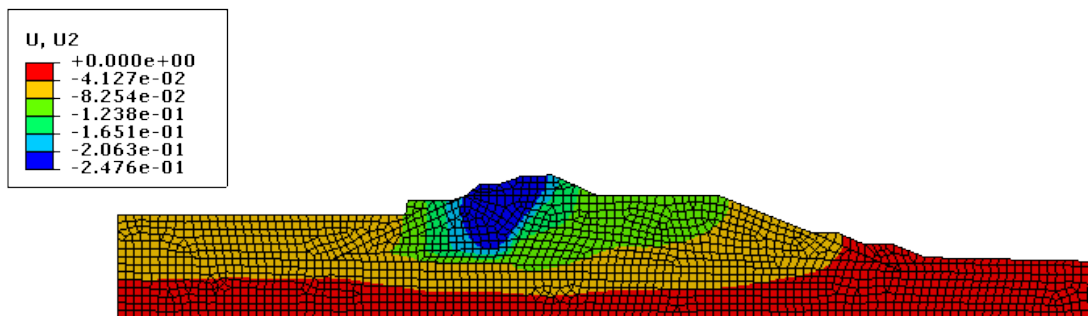


Figure 7. Vertical deformation of USFD 1994 earthquake

Conclusions

Four well published dam case histories distressed during 1971 San Fernando earthquake and 1994 Northridge earthquake are analyzed with the help of the finite element model and based on the relationships proposed by Singh (2012) for yield (anisotropic) shear strength and residual (isotropic) shear strength. 2-D plane strain, four node solid element and DP soil model were used for the preparation of numerical model for all four cases. The horizontal and vertical deformation of four case histories obtained from the finite element analysis comparable with observed performance of these cases.

References

- Bardet JP, Davies, CA. Performance of San Fernando Dams during 1994 Northridge Earthquake. *J Geotech. and Geoenviron. Engrg.* 1996; **122**: 554-63.
- Castro G, Seed RB, Keller TO, Seed HB. Steady-state strength analysis of Lower San Fernando Dam slide. *J. of Geotech. Engrg., ASCE*, 1992; **118**(30): 406-427.
- Huynh P, Schultz M, Wallace L. Re-evaluation of the seismic performance of upper san fernando dam from undriend shear strength. *Proc., Asso., of state dam safety officials conf.*, Boston, MA.: 2006.
- de Alba, P Ballestero, TP. Residual shear strength after liquefaction: A rheological approach, *Journal of Soil Dyn. and Earthq. Engrg.* 2006; **26**: 143-151.
- Jafferries M, Been K. *Soil liquefaction– A critical state approach*, New York, Taylor & Francis, ISBN13: 978-0-203-30196-8: 2006
- Idriss IM., Boulanger, RW. 2008. *Soil Liquefaction During Earthquakes, EERI, MNO-12.*
- Lunne T, Robertson PK, Powell JJM. *Cone penetration testing in geotechnical practice. Blackie Academic, EF Spon/Routledge Publ.* 1997; 312.
- Stark, TD. Mesri, G. Undrained shear strength of liquefied sand for stability analysis. *J. Geotech. Engrg.*, 1992; **118**: 1727-1747.
- Seed HB, Lee KL, Idriss IM, Makdisi FI. The slides in the San Fernando dams during the earthquake of February 9, 1971. *J. of Geotech. Engrg., ASCE* 1975; **11** (7): 651-688.
- Singh R. *Yield and residual shear strengths of non-plastic soils in rapid loading from back analysis.* PhD Dissertation, IIT Kharagpur, India: 2012.
- Simulia Inc. *ABAQUS commercial finite element software package ver. 6.8.* 2008.